Electronic Supplementary Material (ESI) for ChemComm.

pH Stimuli-Disaggregated BODIPY: An Activated Photodynamic/Photothermal Sensitizer Applicable to Tumor Ablation

Yongchao Liu, Chengyan Xu, Lili Teng, Hong-Wen Liu, Tian-Bing Ren, Shuai Xu, Xiaofeng Lou, Haowei Guo, Lin Yuan, Xiao-Bing Zhang*

State Key Laboratory of Chemo/Biosensing and Chemometrics, College of Chemistry and Chemical Engineering, Collaborative Innovation Center for Chemistry and Molecular Medicine, Hunan University, Changsha, 410082. P. R. China.

Reagents and Apparatus. All chemicals were purchased from commercial suppliers and used without further purification. LysoTracker Green was purchased from Beyotime Biotechnology. An appropriate amount of probe PTS was dissolved into DMSO to prepare a stock solution (1 mM). Water was purified and doubly distilled by a Milli-Q system (Millipore, USA). The UV-Visible absorption spectra were acquired via Shimadzu UV-2600 UV-VIS-NIR spectrophotometer. Fluorescence spectra were recorded on a HITACHI F4600 fluorescence spectrophotometer with a 1 cm standard quartz cell. Mass spectra were performed using an LCQ Advantage ion trap mass spectrometer (Thermo Finnigan). NMR spectra were recorded on a Bruker DRX-400 spectrometer using TMS as an internal standard. Thin layer chromatography (TLC) was conducted using silica gel 60 F254 and column chromatography was carried out over silica gel (200-300 mesh), which were obtained from Qingdao Ocean Chemicals (Qingdao, China). The pH was measured with a Mettler-Toledo Delta 320 pH meter. Fluorescence images of cells were obtained from Olympus FV1000-MPE laser scanning confocal microscope (Japan). Photothermal imaging was measured via a thermal infrared imager (FLIR E40). The fluorescent images of mice and serum were obtained via an IVIS Lumina XR Imaging System (Caliper, U.S.A.) equipped with a cooled charge coupled device (CCD) camera. Circular ROIs were drawn over the areas and quantified by Lumina XR Living Image software, version 4.3.

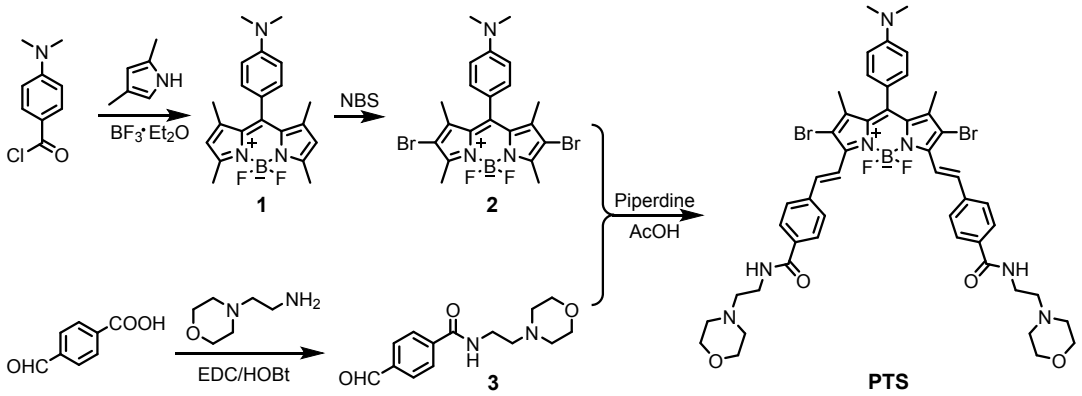

Scheme S1 The synthetic route of PTS.

Compound 1 and compound 2 were synthesized according to the reported literature.

Synthesis of compound 3. *p*-Hydroxybenzaldehyde (1.22 g, 10 mmol), 2-morpholin-4-ylethanamine (1.30 g, 10 mmol), EDCI (1.91 g, 10 mmol) and HOBt (1.35 g, 10 mmol) was dissolved in dichloromethane, and the mixture was stirred at room temperature for 10 h. Then washed with water and saturated sodium chloride aqueous solution and dried with anhydrous sodium sulfate, the product was purified by flash column chromatography by silica gel using dichloromethane/MeOH. ^{1}H NMR (400 MHz, DMSO) δ 10.08 (s, 1H), 8.63 (t, *J* = 5.5 Hz, 1H), 8.04-7.97 (m, 4H), 3.61-3.53 (m, 4H), 3.41 (dd, *J* = 12.9, 6.7 Hz, 2H), 2.50-2.46 (m, 2H), 2.45-2.33 (m, 4H).

Synthesis of PTS. Compound 2 (525 mg, 1 mmol) and compound 3 (655 mg, 2.5 mmol) was dissolved in 10 mL anhydrous acetonitrile under N_2 atmosphere in a two-neck flask. Then piperidine (1.0 mL) and glacial acetic acid (0.6 mL) was introduced into the flask through a syringe. The reaction mixture was stirred at 85 °C for 4 h. Then the solvent was removed under reduced pressure and purified by flash column chromatography over silica gel using dichloromethane/hexane as the eluent to obtain the desired product as a dark-blue solid. ^{1}H NMR (400 MHz, $CDCl_3$) δ 8.12 (d, *J* = 12 Hz, 2H), 7.85 (d, *J* = 7.8 Hz, 4H), 7.78 (d, *J* = 12 Hz, 2H), 7.70 (d, *J* = 7.8 Hz, 4H), 7.15 (s, 2H), 7.05 (d, *J* = 8.1 Hz, 2H), 6.80 (d, *J* = 8.1 Hz, 2H), 3.77 (s, 8H), 3.59 (d, *J* = 4.9 Hz, 4H), 3.06 (s, 6H), 2.68 (t, *J* = 5.2 Hz, 4H), 2.58 (s, 8H), 1.55 (s, 6H). ^{13}C NMR (100 MHz, $CDCl_3$) δ 165.91, 150.09, 146.43, 141.54, 140.97, 138.85, 136.34, 133.45, 132.24, 128.04, 128.04, 126.59, 126.59, 126.52, 126.52, 120.10, 120.10, 118.94, 118.94, 111.29, 111.29, 109.43, 65.70, 65.70, 56.03, 56.03, 52.30, 52.30, 39.21, 39.21, 35.03, 35.03, 13.18, 13.18.

Singlet Oxygen Detection. The singlet oxygen capture agent 1,3-diphenlisobenzofuran (DPBF) was employed to evaluate the singlet oxygen generation. PTS (5 μM) was mixed with DPBF at a final concentration of 50 μM in DMSO or DMSO/TFA. The solutions were irradiated under a 660 nm laser for different times and the absorbance spectra of the mixture solution were monitored immediately. Then, the slope of absorbance of DPBF at 415 nm versus irradiation time was measured.

Photothermal effect and photostability. For PTS in DMSO solutions, 0.1 mL of the

mixtures was irradiated for 480 s under 600 nm lasers for different times. The concentrations of PTS from 0, 5, 50, 100, 200, 300, 400 to 500 μM and the power of 660 nm lasers from 0.25, 0.50, 0.60 to 0.75 W/cm^2. For PTS in DMSO/PBS buffer solutions (DMSO/PBS=1/1, v/v, pH 4.0 and 7.4), 0.1 mL of the mixtures was irradiated for 480 s under 600 nm lasers for different times. The concentrations of PTS are 5 and 50 μM, while the power of 660 nm lasers from 0.25, 0.50, 0.60, 0.68 to 0.75 W/cm^2. Meanwhile, the temperature of solutions was recorded using a thermometer at an interval of 30 s. To evaluate the photostability, PTS (50 μM) in DMSO/PBS buffer solutions were irradiated by 660 nm laser exposure at 0.68 W/cm^2 for 6 min and then cooled in the room temperature for 6 min.

Cell culture and intracellular distribution. 4T1 cells were maintained in RPMI-1640 medium with 10% fetal bovine serum (FBS, GIBCO) and 1% penicillin-streptomycin at 37 °C in a humidified atmosphere containing 20% O_2 and 5% CO_2 as the normoxic condition. When the cell density reached 90% of confluence, a subculture was performed and the medium was changed approximately every day. Cells were seeded in a 20 mm glass-bottom dish plated and grown to around 80% confluency for 24 h before the experiment. Then, the cells were treated with PTS (5.0 μM) and LysoTracker Red (100 nM) for 30 min incubation at 37 °C, the cells were washed with PBS, followed by fluorescence imaging of cells using an Olympus FV1000 MPE laser scanning microscope (Japan) with a 60× oil immersion objective lens. The fluorescence signal of cells incubated with PTS was collected in the channel (650-750 nm) by using a semiconductor laser at 635 nm as the excitation source and LysoTracker Green was collected in the channel (500-550 nm) by using a semiconductor laser at 488 nm as the excitation source.

Detection of intracellular ROS formation. PTS-mediated singlet oxygen production in 4T1 cells was detected by using singlet oxygen indictor DCFH-DA according to the manual. Briefly, 4T1 cells were seeded in 15-mm cell dishes, and then cells were incubated with PTS and DCFH-DA for 30 min. The cells were washed three times with PBS to allow sufficient removal of non-uptake DCFH-DA, and irradiated with 660 nm laser for 0 or 1 min at a power dose of 0.60 W/cm^2. Then, confocal

fluorescence imaging was performed to give the level of intracellular singlet oxygen with the excitation wavelength of 488 nm and 635 nm, emission wavelength from 500 nm to 550 nm, 650nm to 750 nm, respectively.

***In vitro* photocytotoxicity.** Cytotoxicity assays were carried out using 4T1 cells. 5000 cells per well were seeded in a 96-well plate and incubated for 12 h in a humidified incubator for adherence. PTS were dissolved in DMSO, and the solution was then added to cells. After 4 h incubation, the cells were irradiated with a 660 nm pulsed laser to induce phototoxicity. For different treatments, 4T1 cells upon treatment with different concentrations of PTS under irradiation of 660 nm laser (0.5 W/cm^2, 90 s), upon treatment with PTS (10 μM) under irradiation of 660 nm laser (0.5 W/cm^2) for different time or upon treatment with PTS (10 μM) under different power of 660 nm laser for 90 s. Then CCK-8 reagent diluted by RPMI-1640 (FBS free) medium (10%) was added to each well after the removal of culture media and incubated for 0.5 h. Following that, the absorbance was measured at 450 nm on a plate reader Synergy 2 Multi-Mode Microplate Reader (Bio-Tek, Winooski, VT).

4T1 Tumor Model. All animal procedures were performed in accordance with the Guidelines for Care and Use of Laboratory Animals of Hunan University and experiments were approved by the Animal Ethics Committee of College of Biology (Hunan University). About 10^6 4T1 cells were grafted into a BALB/C mouse. Tumors with diameters of around 10 mm were formed after 20 and 30 days, respectively. The fluorescent images of mice were obtained via an IVIS Lumina XR Imaging System (Caliper, U.S.A.) equipped with a cooled charge coupled device (CCD) camera with the collected channel (Cy 5.5).

***In vivo* infrared thermography, histological staining and anticancer efficacy.** To monitor the *in vivo* hyperthermia at tumor, the BALB/C mice were separated into seven groups: Group 1: PTS (pH 4.0) + irradiation, Group 2: PTS (pH 7.4) + irradiation, Group 3: PTS (pH 4.0) + dark, Group 4: PTS (pH 7.4) + dark, Group 5: PBS (pH 4.0) + irradiation, Group 6: PBS (pH 7.4) + irradiation and Control group. Then DMSO/PBS buffer solutions (DMSO/PBS=1/1, v/v, pH 4.0 and 7.4) with or without PTS (0.5 mg/kg) were intratumor injected into the mice bearing 4T1 tumor,

respectively. Then, the tumors suffered from 660 nm laser exposure at 0.68 W/cm^2 or in dark for 5 min. Meanwhile, the temperature at the tumor was recorded using an infrared camera (FLIR E40). Afterwards, the tumor tissues of different groups were extracted at 6 h post-irradiation and then the tissue sections with 10 μm thickness were made in a cryostat, followed by the haematoxylin and eosin (H&E) staining. Finally, the sections were observed using the Digital Slice Scanning System (Pannoramic MIDI). The tumor volumes were calculated through the measurements of their widest and longest dimensions. Finally, the tumors were extracted for taking photos after 15 days treatments.

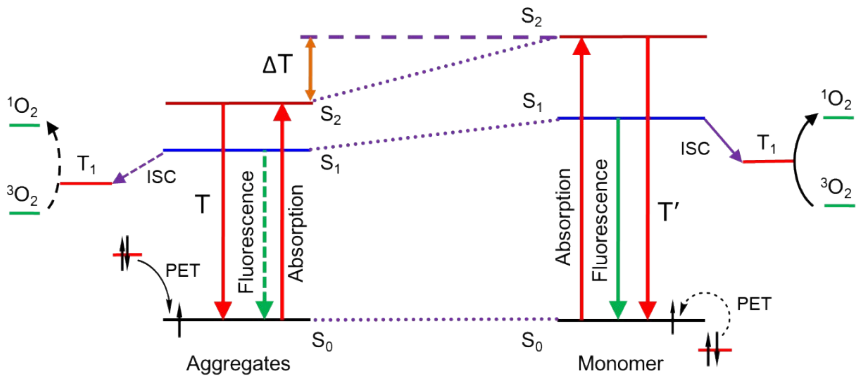

Scheme S2 Stylized Jabłoński diagram for revealing the mechanism of activated PDT and PTT. S0: ground state. S1: excited electronic state. S2: vibrational electronic state. T1: excited triplet state. T and T ′ represent the photothermal effect of the PTS in the aggregate state and the monomer state, respectively. ISC: intersystem crossing. Solid arrows indicate the occurred processes, and dashed arrows indicate the inhibited processes.

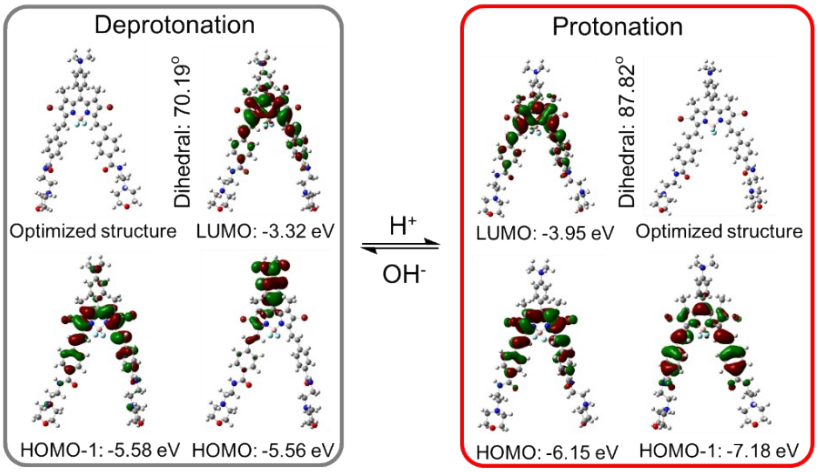

Fig. S1 DFT optimized structures and molecular orbital plots (LUMO, HOMO and HOMO-1) of PTS in its deprotonation and protonation states. Exchange functional: B3LYP. Basis sets: 6-31G*.

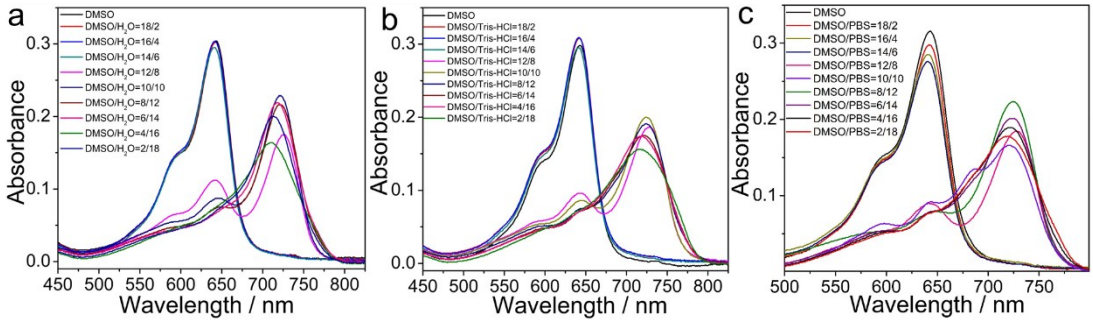

Fig. S2 Normalized absorption spectra of PTS (5 μM) in different proportions of (a) DMSO/H_2O solution (b) DMSO/Tris-HCl solution (pH 7.4) (c) DMSO/PBS solution (pH 7.4).

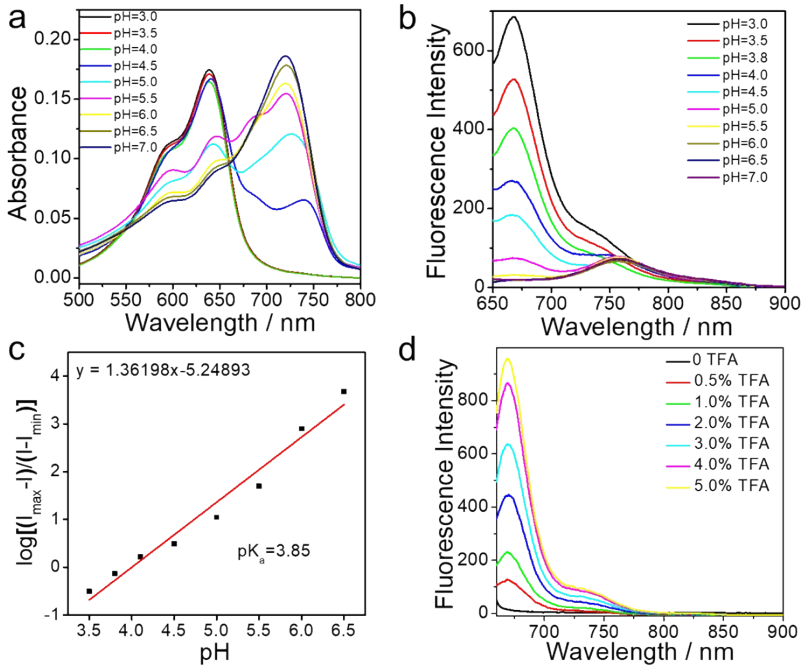

Fig. S3 (a) Absorption and (b)fluorescence spectra of PTS (5 μM) in PBS buffer solution with pH from 3.0 to 7.0. (c) The linear relationship between $\log[(I_{max} - I)/(I - I_{min})]$ and pH (3.5-6.5). (d) Fluorescence spectra of PTS (5 μM) in DMSO solution with different proportions of trifluoroacetic acid (TFA).

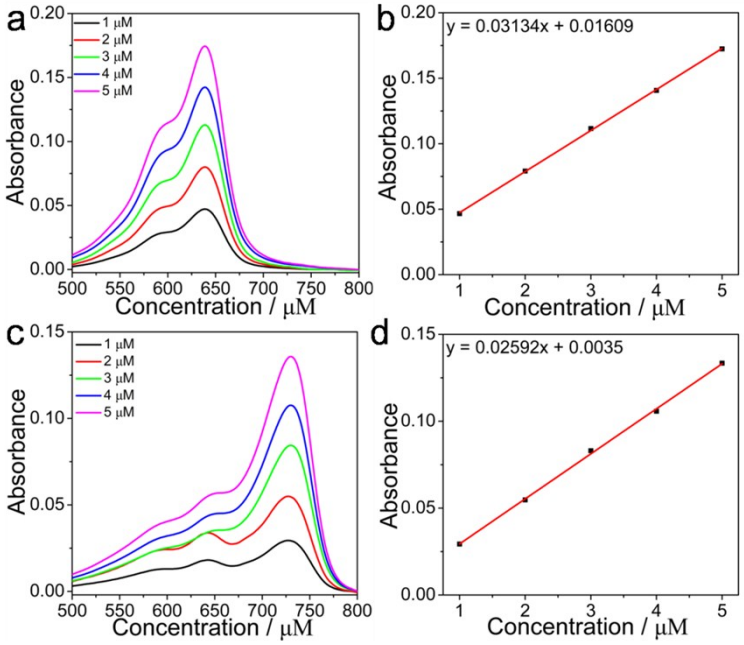

Fig. S4 (a) Absorption spectra of PTS in buffer solution (DMSO/PBS=1/1, v/v, pH 4.0) at various concentrations. (c) Absorption spectra of PTS in buffer solution (DMSO/PBS=1/1, v/v, pH 7.4) at various concentrations. Linear relationship seen in plots of the absorbance at (b) 643 nm and (d) 724 nm vs PTS concentration.

Table S1 Photophysical properties of PTS.

pH	λ_{abs}(nm)	λ_{em}(nm)	**Stokes shift**(nm)	**Ɛ (M^{-1} cm^{-1})**	**State**
4.0	**643**	**667**	**24**	3.314×10^4	**Monomer**
7.4	**722**	**748**	**26**	2.592×10^4	**Aggregate**

All values measured were determined in buffer solutions (DMSO/PBS=1/1, v/v). λ_{abs}: absorption maximum wavelength (nm). λ_{em}: emission maximum wavelength (nm). ε: molar extinction coefficient.

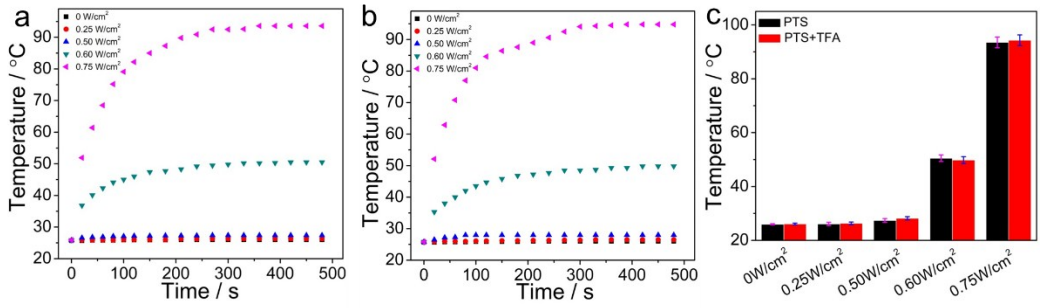

Fig. S5 Photothermal properties of PTS (0.2 mM) in (a) DMSO solutions and (b)

DMSO solutions with 5% trifluoroacetic acid at different powers upon irradiation at 660 nm. (c) Quantitative temperature in (a) and (b).

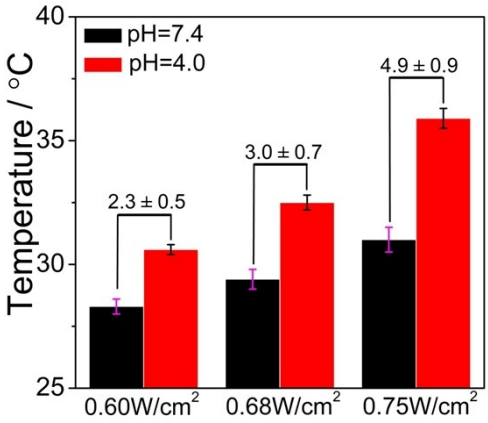

Fig. S6 Temperature changes of PTS (5 μM) in buffer solution (DMSO/PBS=1/1, v/v, pH 4.0 or 7.4) at different powers upon irradiation at 660 nm.

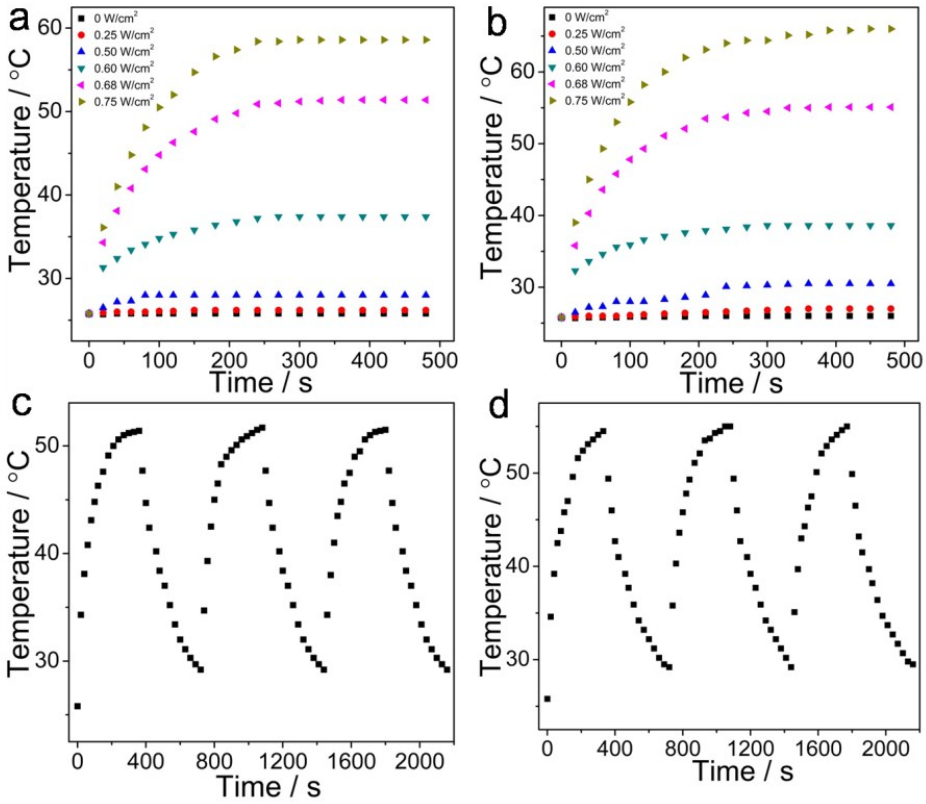

Fig. S7 Photothermal properties of PTS (50 μM) in (a) DMSO/PBS=1/1, v/v, pH 7.4 and (b) DMSO/PBS=1/1, v/v pH 4.0 buffer solutions at different powers upon irradiation at 660 nm. Curves showing the temperature change of PTS in (c) DMSO/PBS=1/1, v/v, pH 7.4 and (d) DMSO/PBS=1/1, v/v pH 4.0 buffer solutions over several ON/OFF cycles involving irradiation with a 660 nm laser (0.68 W/cm2)

for 8 min followed by passive cooling.

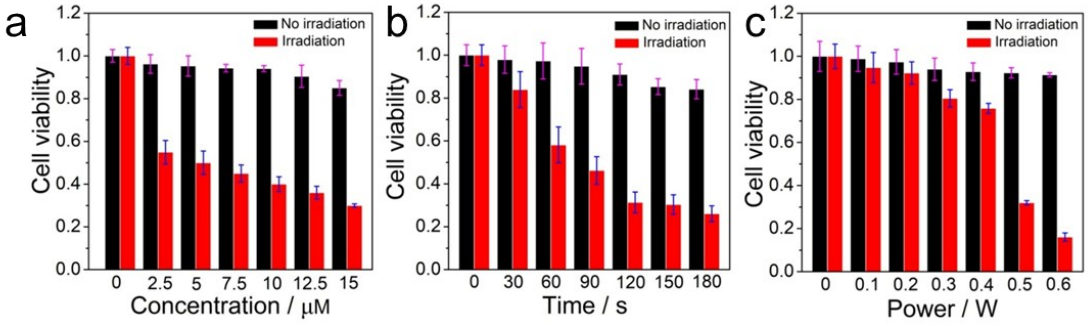

Fig. S8 Cell viability of 4T1 cells (a) upon treatment with different concentrations of PTS under irradiation of 660 nm laser (0.5 W/cm^2, 90 s) or in dark, (b) upon treatment with PTS (10 μM) under irradiation of 660 nm laser (0.5 W/cm^2) for different time, (c) upon treatment with PTS (10 μM) under different power of 660 nm laser for 90 s.

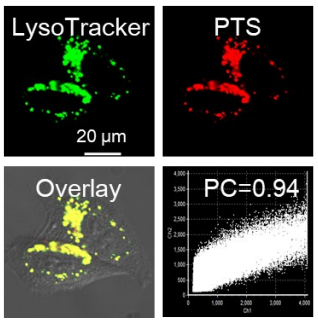

Fig. S9 Confocal fluorescence images of PTS co-localized with LysoTracker Green in 4T1 cells. 4T1 cells were incubated with PTS (5 μM) for 30 min and then with LysoTracker Green (100 nm) for 15 min. Green channel: λ_{ex}=543 nm, λ_{em}= 560-620 nm, Red channel: λ_{ex}= 635 nm, λ_{em}= 655-755 nm. Scale bar: 20μm.

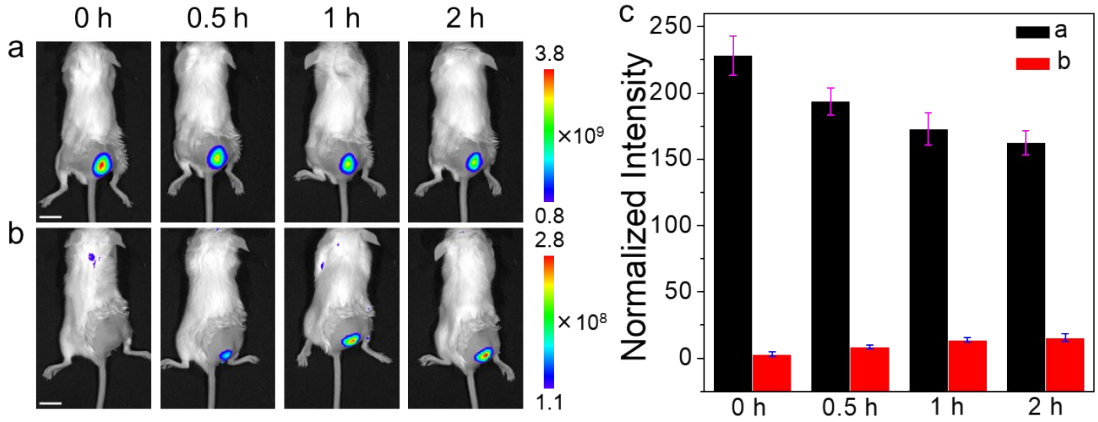

Fig. S10 In vivo fluorescence imaging of 4T1 tumor xenografted mice. The mice were intratumoral injection of 50 μL PTS (50 μM) in (a) DMSO/PBS=1/1, v/v pH 4.0

buffer solutions and (b) DMSO/PBS=1/1, v/v pH 7.4 buffer solutions PBS for different periods of time (0, 0.5, 1, and 2 h). Scale bar: 1cm. (c) Normalized fluorescence intensity of PTS in tumors of (a) and (b).

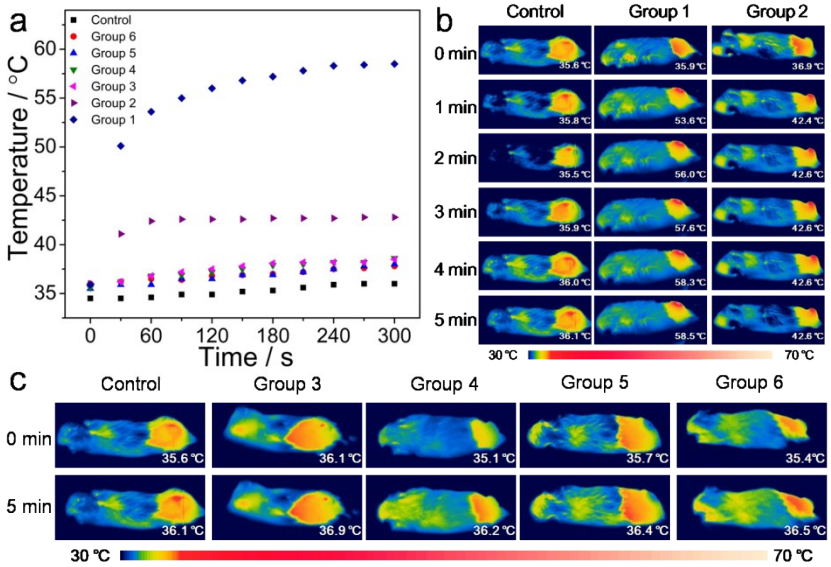

Fig. S11 (a) Photothermal properties of PTS (0.5 mg/kg) in vivo. (b) (c) IR thermal images of BALB/C mice after intratumor injection of PTS after 5 min of 660 nm laser irradiation (0.68 W/cm^2).

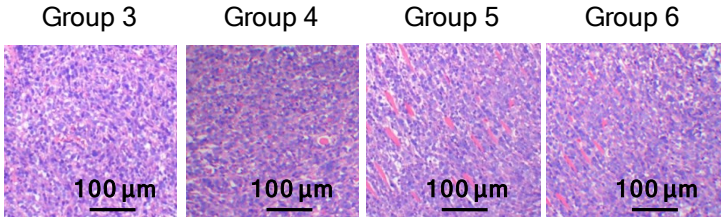

Fig. S12 Histological H&E staining of tumor slices from different groups after treatments. Scale bar: 100 μm.

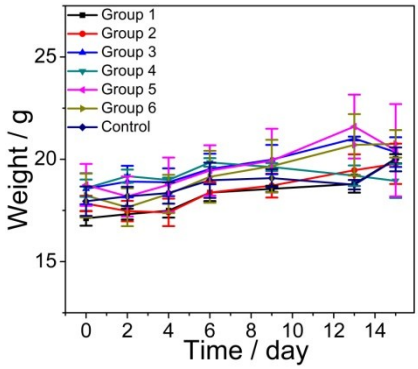

Fig. S13 Changes in body weight of BALB/C mice in each group during phototherapy treatment.

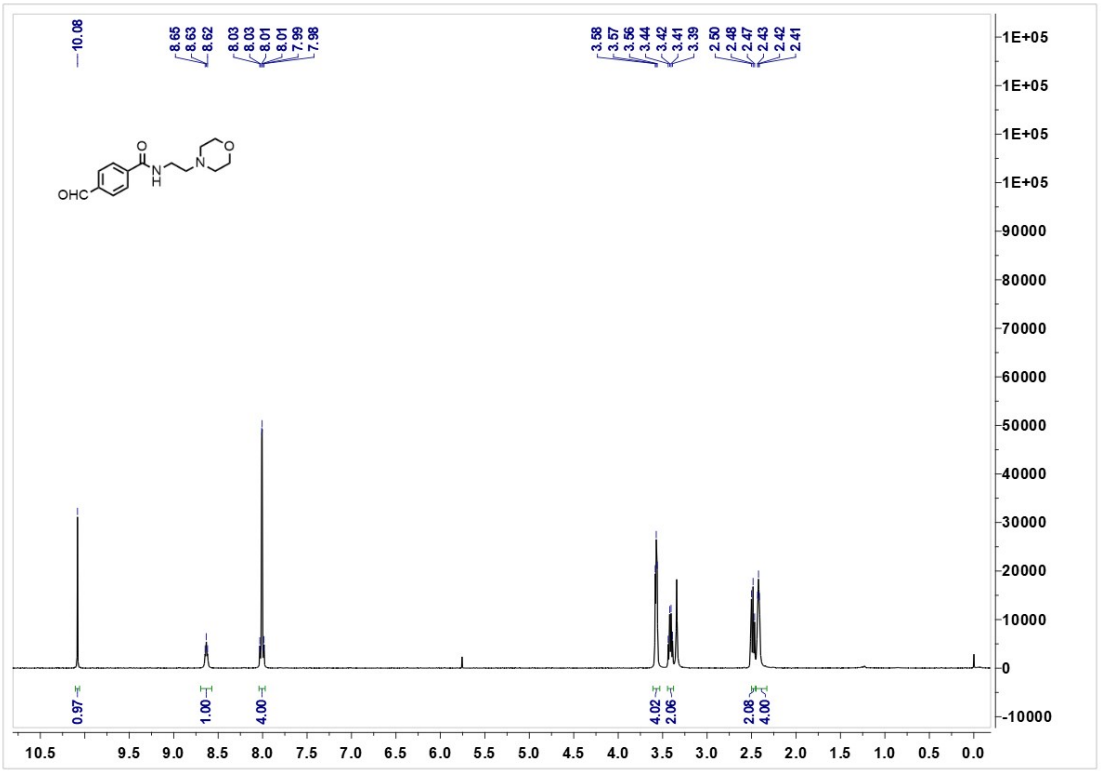

Fig. S14 [1]H NMR spectrum of compound 3.

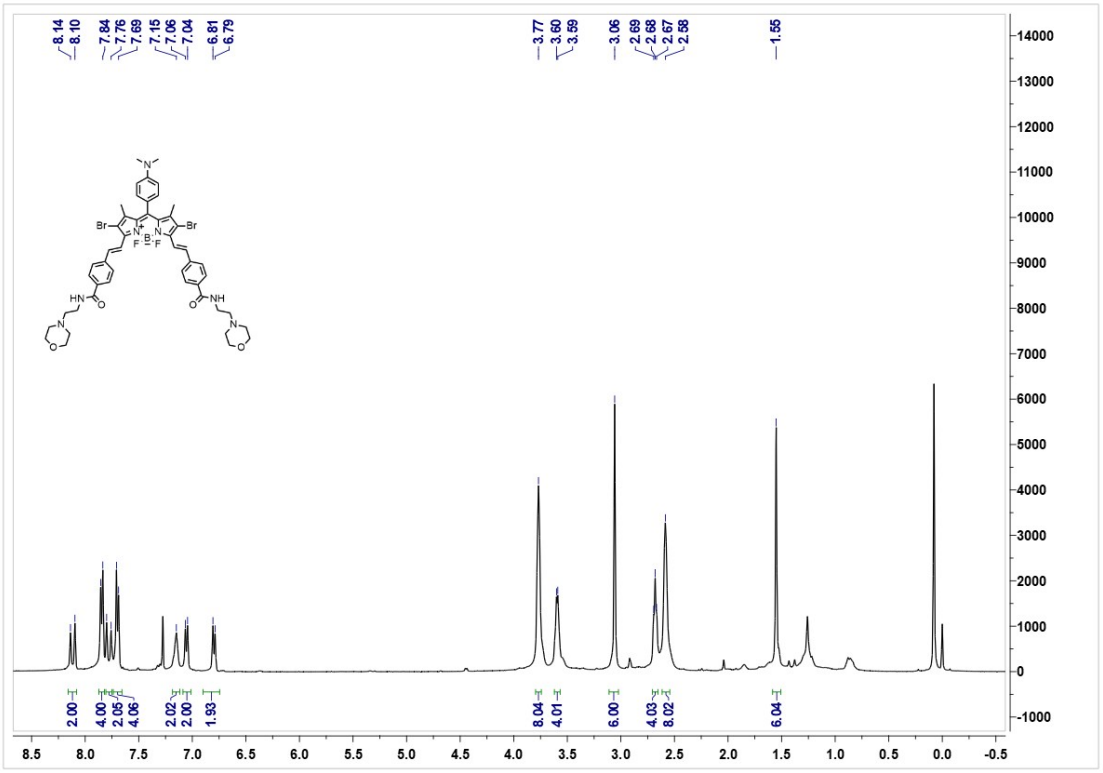

Fig. S15 [1]H NMR spectrum of PTS.

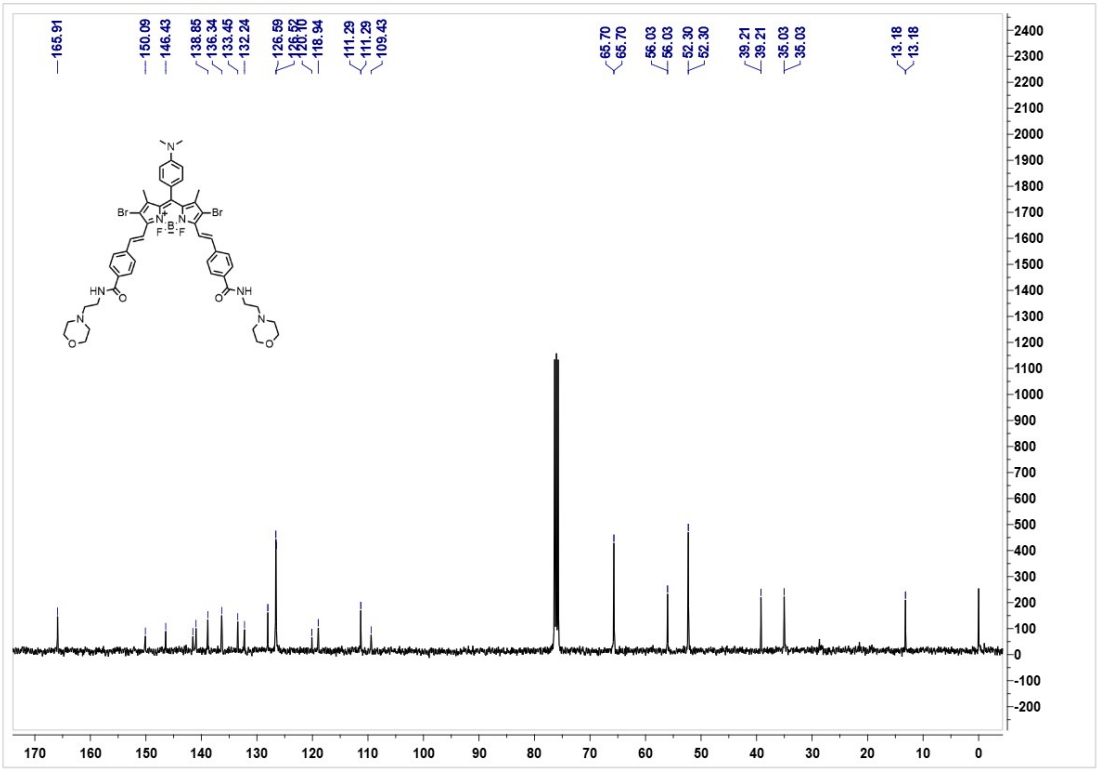

Fig. S16 ^{13}C NMR spectrum of PTS.